U.S. DEPARTMENT OF THE INTERIOR

U.S. GEOLOGICAL SURVEY

HIGH-RESOLUTION SEISMIC-REFLECTION PROFILES AND INTERPRETATION PITFALLS CREATED BY ACOUSTIC ANOMALIES FROM HOLOCENE MUDS BENEATH SOUTH SAN FRANCISCO BAY

by

M.S. Marlow[1], P.E. Hart[1], P.R. Carlson[1], J. R. Childs[1], D.M. Mann[1], R. J. Anima[1], and R.E. Kayen[1]

Open-File Report 94-639

[1]U.S. Geological Survey, Menlo Park, California

1994

High-resolution Seismic-reflection Profiles and Interpretation Pitfalls Created by Acoustic Anomalies from Holocene Muds Beneath South San Francisco Bay

by

M.S. Marlow, P.E. Hart, P.R. Carlson, J. R. Childs, D.M. Mann, R. J. Anima, and R.E. Kayen

ABSTRACT

Very high-resolution (VHR) seismic-reflection profiles were collected in south San Francisco Bay from 1992 to 1994. The initial surveys in 1992 and 1993 utilized a low power (37 Joule) Kaijo SP-3W sonar (4-8 kHz) rigidly mounted to the hull along with an in-line focused cone receiver. Records obtained with this instrument were originally interpreted as showing a complex series of northwest-trending faults offsetting the upper 10-20 m of Holocene bay mud. A subsequent survey in 1994 was run with a towed IKB Seistec profiling system (1-6 kHz), which utilized a higher power (200 Joule) boomer plate source and an in-line focused cone receiver. This instrument generated records of deeper penetration than the SP-3W system and revealed that the reflections originally interpreted as offset by faulting were actually laterally continuous reflection horizons. The interpretation, based on all available data, is that there is not evidence of extensive, young, and near-surface faulting in south San Francisco Bay. A pitfall in interpretation can be explained by comparing seismic-reflection profiles from both systems. The pitfall in the original interpretation was caused by a lateral change in amplitude brightness of reflection events coupled with a long (greater than 15 msec) source signature of the SP-3W system. These effects combined to show apparent offset of reflection packages along sharp vertical boundaries. These boundaries, as shown by the Seistec system, in fact occur where the reflection amplitude diminishes abruptly on laterally continuous reflection events. This dramatic lateral variation in reflection amplitude is attributed to the localized presence of biogenic(?) gas.

Aeromagnetic data and juxtaposition of different rock types on the adjacent onshore San Francisco peninsula do suggest that northwest-trending faults extend across south San Francisco Bay. However, these faults may have ceased major strike-slip motion as early as 4.5 Ma, when Pacific and North American plate motions changed, such that compressional stress became more fault-normal.

INTRODUCTION

The south San Francisco Bay region, as defined here, extends about 50 km south from the San Francisco-Oakland Bay Bridge to San Jose and is surrounded by more than 20 communities housing several million people. The bay is bounded by active faults - the Hayward/Calaveras system to the east and the San Andreas to the west. Regional linear magnetic anomalies and mapped onshore faults trend northwest-southeast and project under the water in the south bay (Figs. 1 and 2). The linear magnetic anomalies were originally interpreted by Brabb and Hanna (1981) to delineate fault trends in the south bay. To study these trends and possible faults, we conducted a series of surveys using very high-resolution seismic-reflection systems to see if young faults ruptured the sedimentary fill beneath the south bay or whether these faults are old and offset only units in bedrock beneath the bay's sedimentary fill.

San Francisco Bay was considered to be partly erosional and partly structural in origin by Lawson (1914). His boundaries for the Marin-San Francisco block, containing the bay, are bounded by the Hayward and other faults northeast of the bay and the San Bruno and other faults southwest of the bay. The boundaries of the block were changed slightly by Clark (1930), who considered the San Francisco Bay block to be bordered by the Hayward and San Andreas faults, which are the generally accepted boundaries of the block today.

Between the San Andreas and Hayward faults the major structural elements of the San Francisco Bay block are dominated by northwest-trending shear zones and linear magnetic anomalies. The shear zones and faults, best exposed in the upper San Francisco Peninsula, juxtapose a heterogeneous assortment of Mesozoic Franciscan Complex rocks. Two major shear zones in San Francisco trend southeastward toward San Francisco Bay as mapped by Schlocker (1974). The northern of these two shear zones, which he called the Fort Point-Potrero Hill-Hunters Point shear zone, is about 2 km wide and bisects the city of San Francisco. This shear zone extends from Fort Point and the southern abutment of the Golden Gate Bridge to the southeast to Potrero Hill and Hunters Point. Schlocker (1974) speculated, on the basis of aeromagnetic anomalies, that the shear zone extends across San Francisco Bay to the Coyote Hills in the east bay. The shear zone consists of intensely deformed sedimentary, metamorphic and ultramafic rocks that separate Franciscan Complex sandstones and shales to the north, from radiolarian chert and metamorphosed intrusive rocks to the south (Schlocker, 1974).

As mentioned above, aeromagnetic anomalies plus mapped faults, earthquake epicenters, and the distribution of igneous rocks were all used by Brabb and Hanna (1981) to infer several faults in south San Francisco Bay. The most prominent of these, the Hunters Point fault, extends northwest from an inferred fault in the Coyote Hills area near Newark, at least to the Hunters Point area where it projects into the Fort Point-Potrero Hill-Hunters Point shear zone of Schlocker (1974). The Redwood City fault of Brabb and Hanna (1981), extends from Palo Alto northwest to the Coyote Point. This fault is approximately on trend with the Hillside fault mapped by Bonilla (1965) in the South San Francisco area. The Hillside fault is the largest and best exposed fault in a wide zone of sheared Franciscan rocks (Bonilla, U.S.G.S., personal communication, 1993).

Surveys (1992-94)

We conducted two very high-resolution seismic-reflection surveys in 1992 and 1993 in order to investigate the possible offshore extension of the northwest-trending shear zones and faults into south San Francisco Bay (Fig. 3). These reflection surveys collected about 1000 km of high-resolution seismic-reflection data using a Kaijo SP-3W subbottom profiling system. The SP-3W surveys revealed apparent vertical offsets in young (late Holocene) muds of south San Francisco Bay (vertical arrows shown on Fig. 4). The offsets trend northwest, on strike with the northwest-trending shear zones and faults. To further evaluate these apparent offsets, an additional 116 km of high-resolution seismic-reflection data were collected using a IKB Seistec Profiling System. Reflection profiles collected with this system (Fig. 5) gave a much different image of the apparent vertical offsets shown in Figure 4. These new data show continuous reflections that laterally change abruptly in amplitude.

The purpose of this paper is to discuss the possibilities of erroneous interpretations and their implications. We then try to explain the different images and to relate these images to the geology of the south bay sediment.

Equipment

The Kaijo SP-3W seismic-reflection system uses a 37 Joule, 4-8 kHz electromagnetic boomer source and 12° in-line focused cone receiver (hydrophones mounted vertically in cone), which are both rigidly mounted to the sides of a vessel. The SP-3W system, including the in-line focused cone receiver, typically penetrates 5-10 m in the bay muds with an estimated resolution of about 20 cm based on correlation of reflections to cored stratigraphic units.

The IKB Seistec Profiling System, utilizes a towed 200 Joule, 1-6 kHz boomer source and in-line focused cone receiver similar to the Kaijo SP-3W receiver. The Seistec system reportedly resolves sandy mud beds as thin as 25 cm with penetration in excess of 30 m (Simpkin and Davis, 1993). Penetration in San Francisco Bay was typically 5-20 m.

Both seismic reflection data sets were digitally recorded, and navigation was recorded from the Global Positioning System (GPS) in differential mode.

Coring and core logging techniques

Subsurface strata imaged on the very high-resolution (VHR) seismic-reflection profiles were sampled with a 390 kg gravity corer that has a steel core barrel 6 m long and 7.6 cm in diameter. One core (#5; Figs. 3 and 4) penetrated layers imaged by the VHR profiles. Before being split for sampling, the cores were logged for physical properties on a multi-sensor whole core sediment logging device. The logging device was built in Great Britain by Schultheiss Geoteck, Ltd. This device is controlled by a personal-computer driven software system, developed for data acquisition and instrument manipulation. The system logs sediment bulk density, compressional velocity, and magnetic susceptibility of un-split whole sediment cores. These properties are used to develop physical property profiles of the cores.

SEISMIC-REFLECTION DATA

Interpretation of SP3W Line 93-114

Seismic-reflection Line 93-114 (Fig. 4) was collected with the Kaijo SP-3W system about 1 to 2 km northeast of San Francisco International Airport (SFO, Fig. 3). This profile shows three apparent vertical displacements of 2 m near the center and southwest side of the profile (marked by vertical arrows). Three reflections are recognizable in the subbotom: the first is a high amplitude package of about 6 closely spaced "ringy" reflections A (Fig. 4), followed by another package of reflections B about 3 m below the first package, and then a third set of reflections C about 3 m below the second package and just above the multiple (M). These three packages of reflections are offset from adjacent packages along apparent vertical, knife-edge breaks. The breaks were originally interpreted as fault offsets because the reflection sequences lined up in reconstructions made by cutting a copy of the records and sliding the pieces along the vertical breaks (highlighted by vertical arrows on Fig. 4). However, reflections from above reflection A near the middle of the profile appear to extend laterally across one of the knife-edge

breaks. A problem with the fault interpretation was how to maintain these sharp fault scarps in an estuarine environment, strongly influenced by tidal fluctuations without showing signs of erosion and infilling if they were indeed faults that intersected the bay floor. To further evaluate these apparent breaks, we surveyed some of the south bay using a IKB Seistec seismic-reflection profiling system.

Interpretation of Seistec Line 94-112A

Seistec Line 94-112A (Fig. 5) was collected about 3 km northwest of the SP-3W Line 93-114 along a northeast-southwest transect (Fig. 3). This profile shows a series of three high-amplitude subbottom reflections that dip gently to the northeast. The shallowest reflection A is brightest in amplitude near the northeastern end of the profile. This reflection can be traced laterally to the southwest and dims abruptly in amplitude where a deeper reflection B abruptly brightens in amplitude. This second reflection can be traced laterally to the southwest to where the second reflection suddenly dims in amplitude and a third deeper reflection C suddenly brightens in amplitude. All three reflections can be traced laterally, suggesting unbroken stratigraphic continuity of all three reflections. The interesting characteristic of all three reflections is the lateral brightening and dimming of these stacked reflections. This characteristic is important in comparing the Seistec data to the SP-3W data.

Seistec line 94-109 (Fig. 6) was collected near the SP-3W Line 93-114. Near the center of the profile there are several stacked reflections that dip gently to the northeast like the section along Seistec Line 94-112A (Fig. 5). The northeast-dipping reflections here change amplitude laterally, brightening and dimming along the line similar to the reflections on Seistec Line 94-112A, .

INTERPRETATION PITFALLS

We re-examined the "fault" offsets interpreted on the SP-3W Line 93-114 because of the lateral continuity of northeast-dipping reflections shown in the Seistec profiles. We split the profile (Fig. 7) along one of the sharp vertical offsets and inserted the outgoing source signature of the SP-3W system that was recorded in the water column of a nearby shipping channel. The outgoing pulse of the SP-3W is at least 15 msec long with at least two prominent peaks that follow the initial pulse. By carefully matching the source signature to the bright reflection A in Figure 7, we see that reflections B and C match up with peaks in the outgoing pulse and are therefore artifacts. Where a strong reflection (A in Fig. 7) abruptly dims along the SP3W profiles, allowing the imaging of a deeper bright reflection (A'), this deeper reflection creates a reflection package identical to A. Shifting A' up to A also aligns B with B' and C with C' and gives the strong impression of reconstructing the "pre-faulting" geology. However, the similar character of A and A' and the positions of artifacts B and C are due to source signature characteristics and not geology. The SP3W low power (37 Joules) does not penetrate beneath the first high amplitude reflection as comparison of the SP3W and Seistec data will show below. As we saw in the Seistec lines, these strong reflections dim and brighten in amplitude but are laterally continuous and stacked above similar reflections that are laterally continuous but abruptly brighten and dim in amplitude. A possible explanation for these dramatic amplitude changes is given in the coring section below.

The acoustic anomalies were originally misinterpreted as fault offsets (Mann et. al, 1993). Following the acquisition of the IKB Seistec profiles in May, 1994, we reexamined all the data collected in south San Francisco Bay. To date, we cannot unequivocally demonstrate any offsets in the Holocene muds beneath the bay. There may be faulting deeper beneath the bay, but these structures, if they exist, will require the use of high-resolution, multichannel seismic-reflection profiles acquired with small airguns as a sound source for deeper penetration than the SP-3W or Seistec systems.

CORING RESULTS

A 4.3 m long core, recovered along SP-3W Line 93-114, penetrated the bright reflection at a subbottom depth of about 2.9-3.0 m (Fig. 4). The bright reflection is from the base of a layer of shell fragments about 15 cm thick overlying inter-laminated sand and silt. The reflection is the result of an impedance contrast that corresponds to changes in density and compressional wave velocity as measured along the core with the core logger (Fig. 8). At a subbottom depth of about 2.5 to 2.6 m there is a marked increase in the density and a decrease in the compressional wave velocity that correspond to the shell layer. The density probably increases because of the concentration of shell material, but the overall density of this section may decrease because of a decrease in matrix density observed in the shell layer. Interestingly, this shell layer corresponds to a lithologic change from predominantly shelly beds inter layered with muddy silt beds above to more sandy, laminated beds without shelly layers below 2.9 m. The upper section, predominantly muddy silt, may act as seal for any gas accumulating in the more porous interbedded sand and silt section below. Such trapped gas may occur in pockets laterally along the beds and is the most likely explanation for the sudden brightening and dimming in the amplitude of reflections on the seismic-reflection records.

DISCUSSION AND CONCLUSIONS

The brightening and dimming in the amplitude of reflections could be attributed to the presence or absence of gas in the sedimentary section. Gas in the sediment, for example, may cause the decrease in compressional wave velocities measured in a core that straddles the reflections of varying amplitude. Domenico (1976) and Singh and others (1993) demonstrated that as little as two percent of the pore space filled with gas in sediment (sediment porosity=60 percent) will lower the compressional velocity from 1.7 to 1.3 km/s. Alternatively, the brightening and dimming of reflection amplitude may be due to lateral changes in lithology of the sedimentary section, affecting the localization of gas. The bright areas, thereby, may correspond to shell mounds that would concentrate gas within reef-like, buried oyster banks. The brightening also may correspond to pockets of sand that localize gas. In any event, we have demonstrated that reflections are laterally continuous and not offset by faulting in the upper 10-20 m of bay mud as originally thought.

The aeromagnetic data and the juxtaposition of different rock types onshore on the San Francisco peninsula do suggest that south San Francisco Bay is underlain by faults. The VHR seismic reflection records indicate that these faults probably do not rupture the upper 10-20 m of bay mud. The deeper faults may have been active prior to 4.5 Ma, when the motion between the Pacific and North American plates was more extensional, allowing strike-slip movement in the south bay. A change to more fault normal compression

occurred about 4.5 Ma (Zoback et. al, 1987), which may have limited slip occurring within the bay block.

REFERENCES

Bonilla, M.G., 1965, Geologic Map of the San Francisco South Quadrangle, California: U.S. Geological Survey Open-file report, map scale 1:20,000.

Brabb, E.E., and Hanna, W.F., 1981, Maps showing aeromagnetic anomalies, faults, earthquake epicenters, and igneous rocks in the southern San Francisco Bay Region, California: U.S. Geological Survey Geophysical Investigations Map GP-932, map scale 1:125,000.

Clark, B.L., 1930, Tectonics of the Coast Ranges of Middle California: Univ. Geological Society of America, v. 41, no. 4, p. 747-828.

Domenico, S.N., 1976, Effect of brine-gas mixtures on velocity in an unconsolidated sand reservoir: Geophysics, v. 41, p. 882-894.

Jachens, R.C. and Roberts, C.W., 1993, Aeromagnetic map of the San Francisco Bay area, California: U.S. Geological Survey Map GP-1007, one sheet.

Jennings, C.W., 1992, Preliminary fault activity map of California, California Dept. of Conservation, Division of Mines and Geology, open-file report 92-03, 1 plate with 77 p. reference appendix.

Lawson, A.C., 1914, Description of the San Francisco district: Tamalpias, San Francisco, Concord, San Mateo and Hayward quadrangles: U.S. Geological Survey Geologic Atlas no. 193, San Francisco folio, map scale 1:62,500.

Mann, G. M., Marlow, M.S., and Brabb, E. E., 1993, Newly discovered strike-slip faults in south-central San Francisco Bay: EOS Abstracts with Program, v. 74, p. 693.

Schlocker, J., 1974, Geology of the San Francisco North Quadrangle, California: U.S. Geological Survey Professional Paper 782.

Simpkin, P. G., and Davis, A., 1993, For seismic profiling in very shallow water, a novel receiver. IKB-SEISTEC profiler (A line-in-cone configuration) yields 0.25 meter resolution in water depths less than 2 meters: Sea Technology, September, 1993, p. 21-28.

Singh, S.C., Minshull, T.A., and Spence, G.D., 1993, Velocity structure of a gas hydrate reflector: Science, v. 260, p. 204-207.

Zoback, M.D., Zoback, M.L., Mount, V.S., Suppe, J., Eaton, J.P., Healy, J.H., Oppenheimer, D., Reasenberg, P., Jones, L., Raleigh, C.B., Wong, I.G., Scott, O., and Wentworth, C., 1987, New evidence on the state of stress of the San Andreas fault system: Science, v. 238, p. 1105-1111.

FIGURE CAPTIONS

Figure 1. Aeromagnetic map of the San Francisco Bay region with principal faults and magnetic anomalies courtesy of R. Jachens (written comm., 1994;

Jachens and Roberts, 1993). Aeromagnetic anomalies (and associated proposed faults) of Brabb and Hanna (1981) denoted as follows: HP - Hunters Point magnetic anomaly; SJ - San Jose magnetic anomaly; RC - Redwood City magnetic anomaly. Contour interval of 100 nanoTeslas (1 nT = 1 gamma).

Figure 2. Quaternary fault map of greater San Francisco Bay region from Jennings (1992). Included in upper San Francisco Peninsula are three Mesozoic shear zones described in text, and denoted as follows (after Schlocker, 1974): FH - Fort Point-Potrero Hill-Hunters Point shear zone (lies within two dotted lines); CC - City College fault (dashed and dotted); CH - Coyote Hills, and H - Hillside fault (dashed). Also abbreviated on map is the Quaternary San Bruno fault - SB (dotted).

Figure 3. Trackline map of 1992, 1993, and 1994 surveys that collected high-resolution seismic-reflection profiles in south San Francisco Bay. Portions of lines 93-114, 94-109, and 94-112A are highlighted and refer to sections of these lines shown in Figures 4, 5, 6, and 7.

Figure 4. High-resolution seismic-reflection profile 93-114 collected with the Kaijo SP-3W seismic-reflection system. Location of profile and core #5 are shown in Figure 3. Note the very sharp apparent offsets, marked with vertical arrows, between groups of reflections A B, and C. The multiple of reflection A is marked with an M.

Figure 5. High-resolution seismic-reflection profile 94-112A collected with the IKB Seistec seismic-reflection system. Location of profile is shown in Figure 3. Note the continuity of reflections A, B, and C above one another as they laterally dim and brighten in amplitude.

Figure 6. High-resolution seismic-reflection profile 94-109 collected with the IKB Seistec seismic-reflection system. Compare this line to profile 93-114 (Fig. 4) collected nearby (Fig. 3). Stacked reflections are continuous reflections that can be traced laterally above one another and are not offset by faulting.

Figure 7. High-resolution seismic-reflection profile 93-114 collected with the Kaijo SP-3W seismic-reflection system showing an inserted full wave form source signature aligned with reflection horizon A. The outgoing pulse was recorded nearby in deeper water. Each source signature trace is the sum of twenty shots and is bandpass filtered to match the data. Note the creation of reflection packages over 15 msec long from bright reflections high in the section.

Figure 8. Physical property profile logs and visual description for Core # 5, including P-wave velocity, bulk density, and magnetic susceptibility measurements.

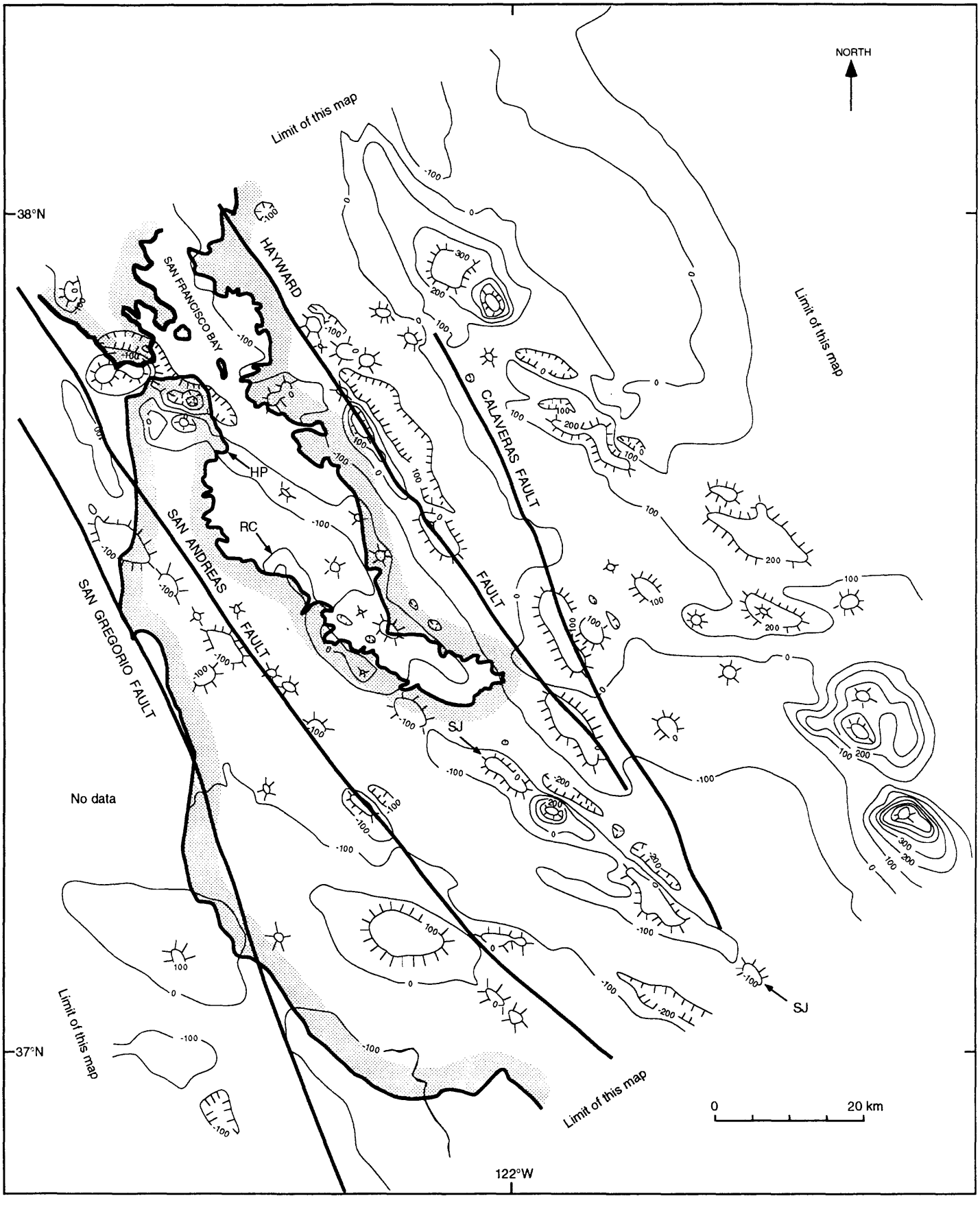
NORTH
Limit of this map
38°N
37°N
122°W
HAYWARD
FAULT
SAN FRANCISCO BAY
CALAVERAS FAULT
HP
RC
SAN ANDREAS FAULT
SAN GREGORIO FAULT
SJ
SJ
No data
Limit of this map
Limit of this map
Limit of this map
0
20 km

Figure 1

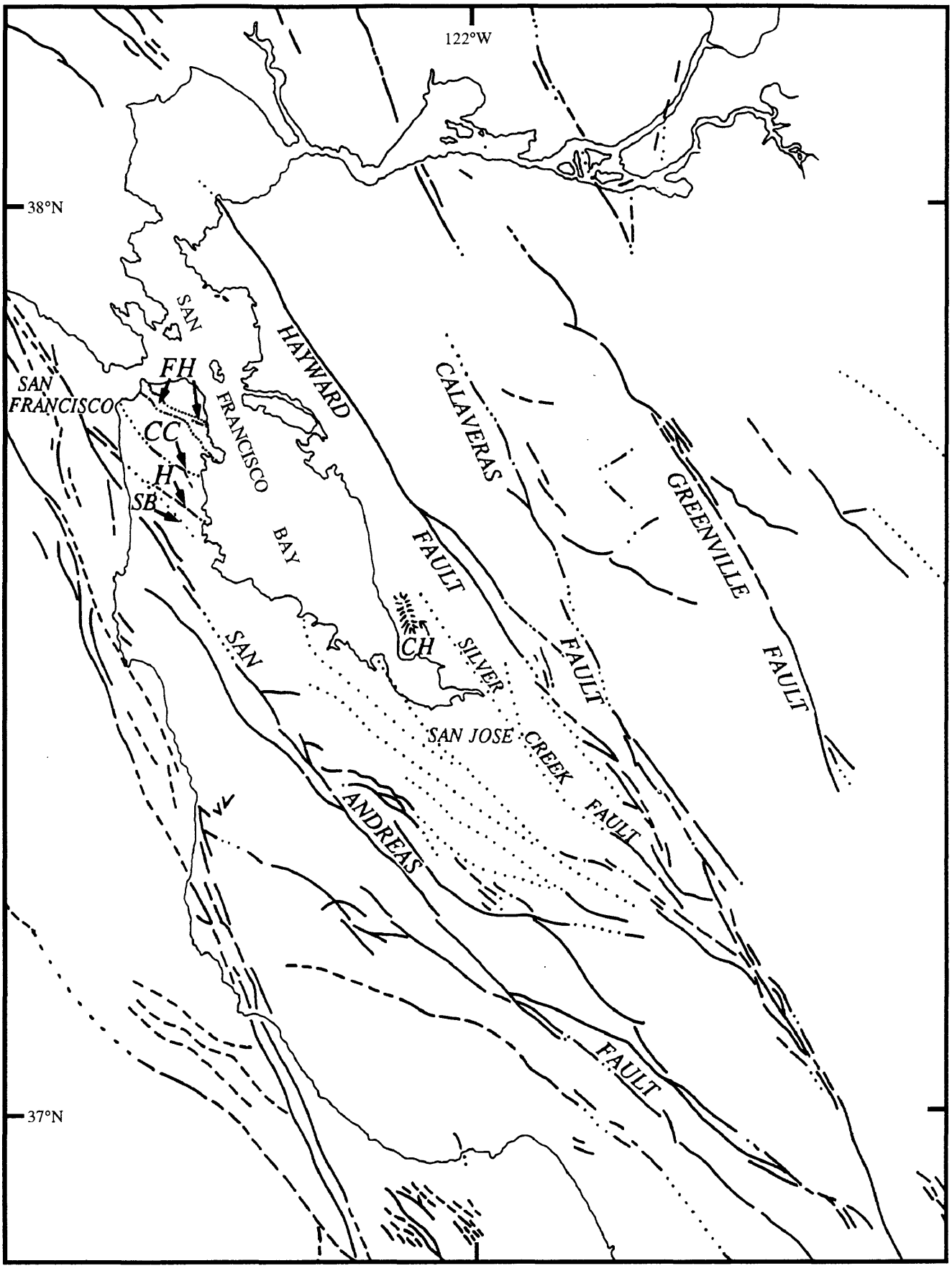
122°W
38°N
37°N
SAN
FRANCISCO
FH
CC
H
SB
SAN
FRANCISCO
BAY
HAYWARD
FAULT
CALAVERAS
FAULT
GREENVILLE
FAULT
CH
SILVER
CREEK
FAULT
SAN JOSE
SAN
ANDREAS
FAULT

Figure 2

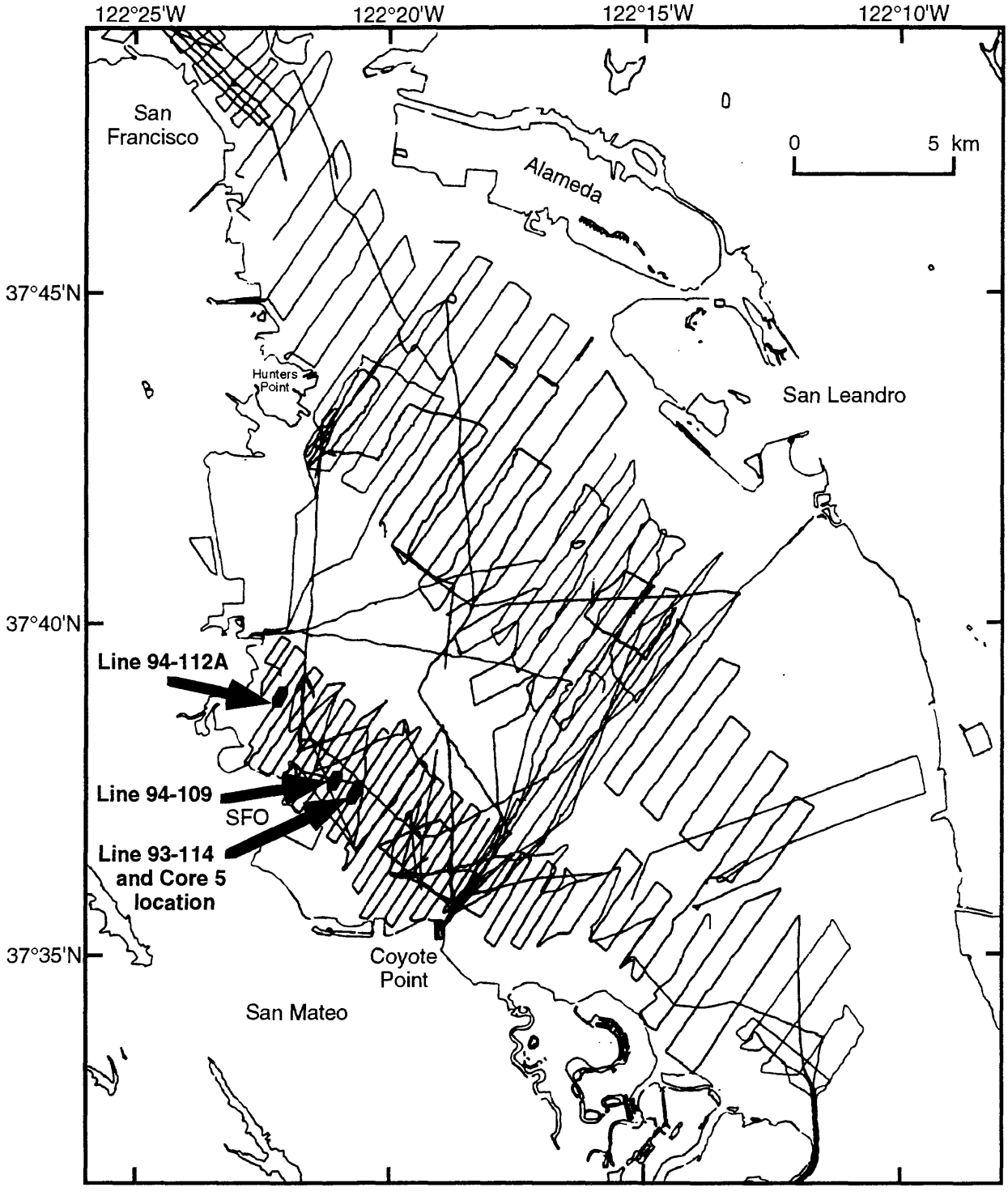
122°25'W
122°20'W
122°15'W
122°10'W
San Francisco
Alameda
0
5 km
37°45'N
Hunters Point
San Leandro
37°40'N
Line 94-112A
Line 94-109
SFO
Line 93-114 and Core 5 location
37°35'N
Coyote Point
San Mateo

Figure 3

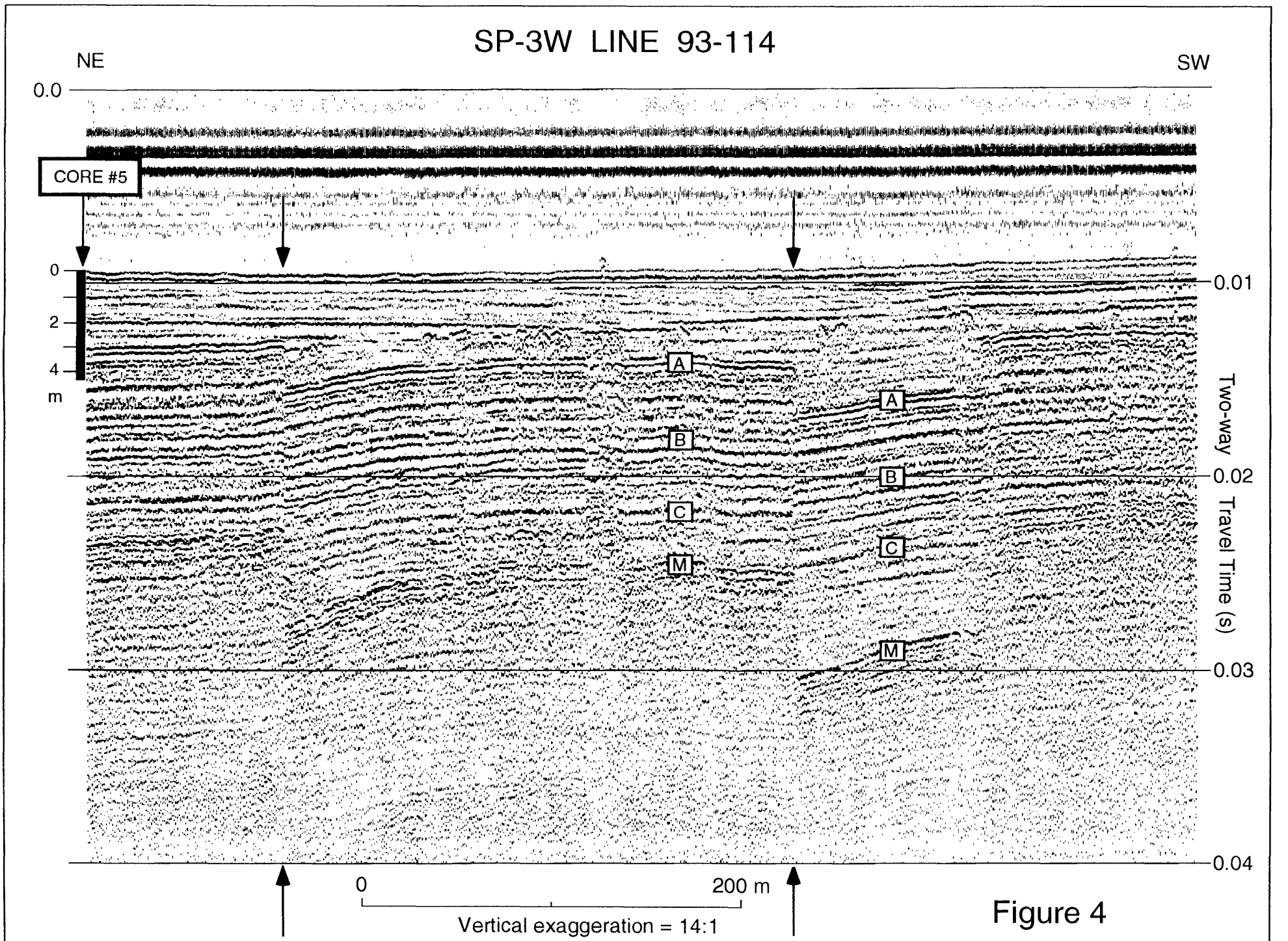
SP-3W LINE 93-114
NE
SW
0.0
CORE #5
0
2
4
m
A
A
B
B
C
C
M
M
0.01
0.02
0.03
0.04
Two-way Travel Time (s)
0
200 m
Vertical exaggeration = 14:1

Figure 4

SEISTEC LINE 94-112A

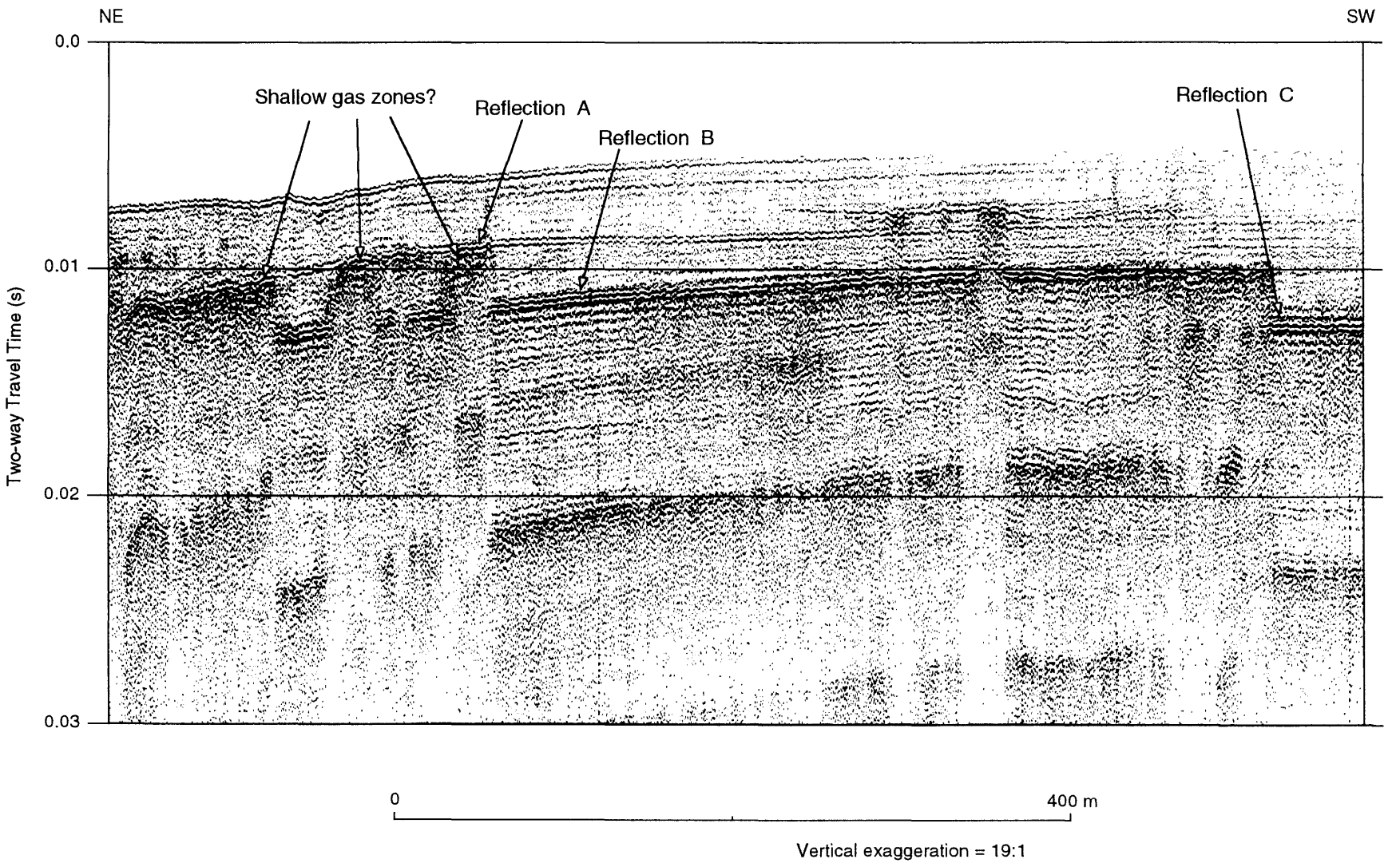

Figure 5

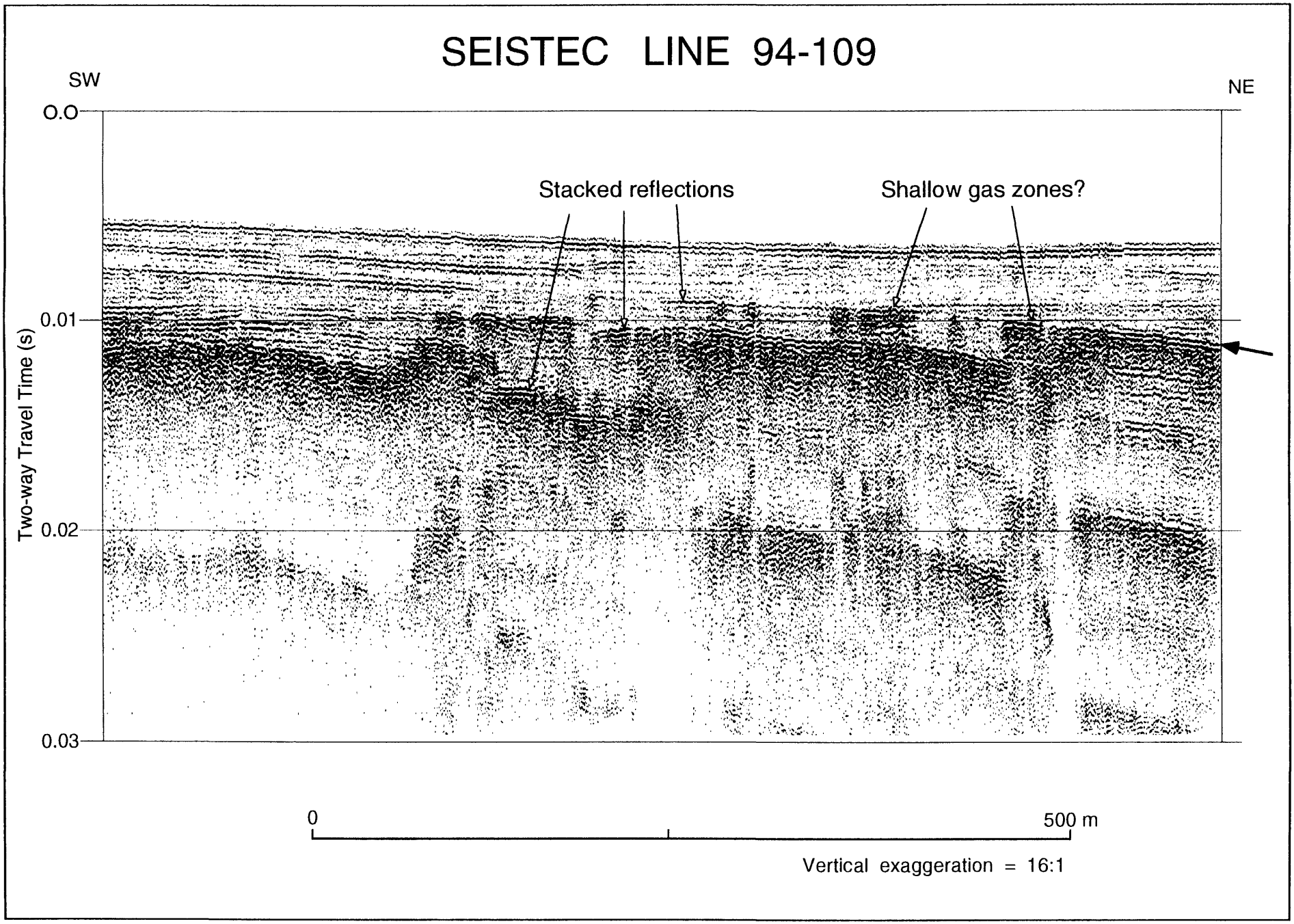
SEISTEC LINE 94-109
SW
NE
0.0
0.01
0.02
0.03
Two-way Travel Time (s)
Stacked reflections
Shallow gas zones?
0
500 m
Vertical exaggeration = 16:1

Figure 6

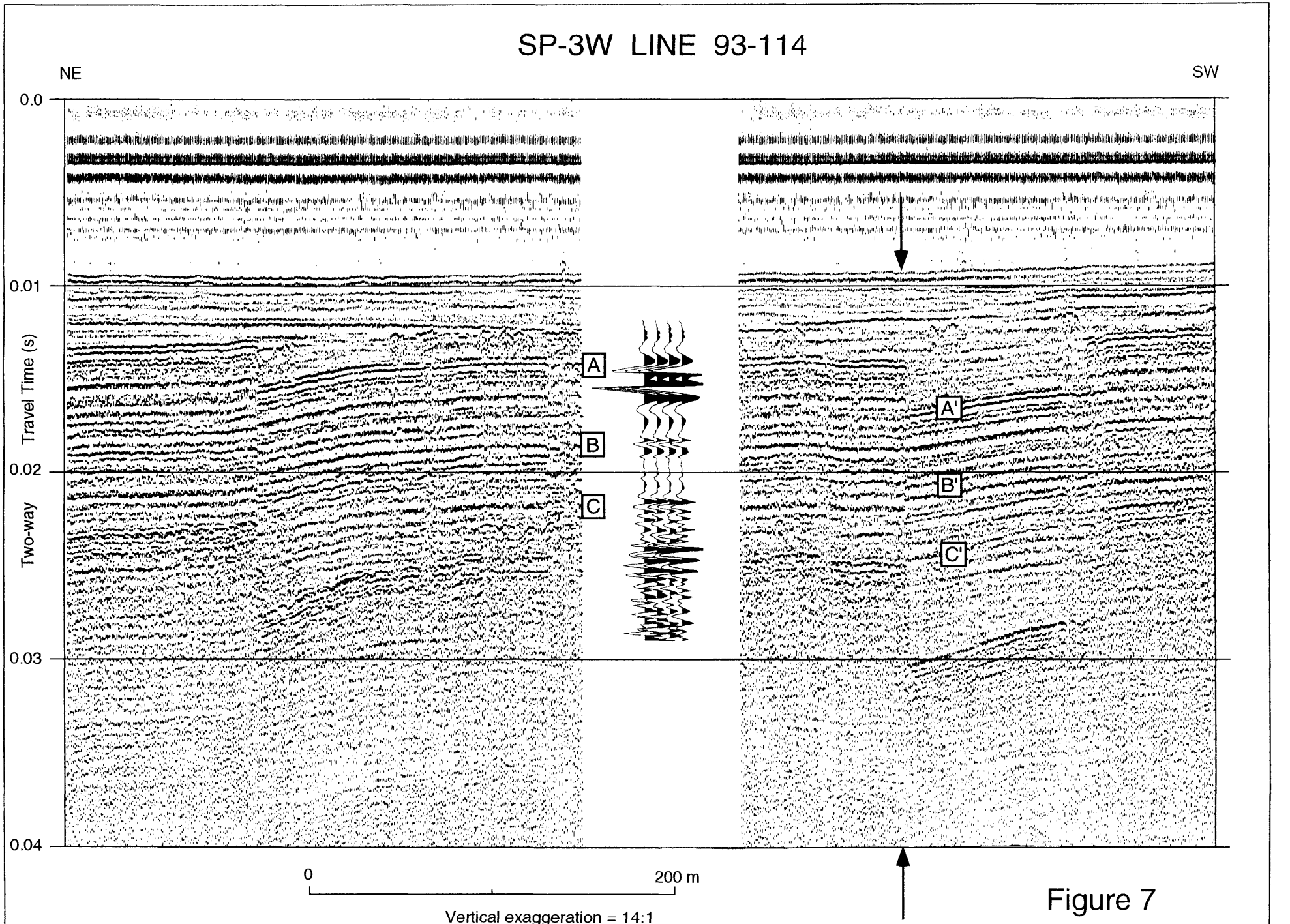
SP-3W LINE 93-114
NE
SW
0.0
0.01
0.02
0.03
0.04
Travel Time (s)
Two-way
A
B
C
A'
B'
C'
0
200 m
Vertical exaggeration = 14:1

Figure 7

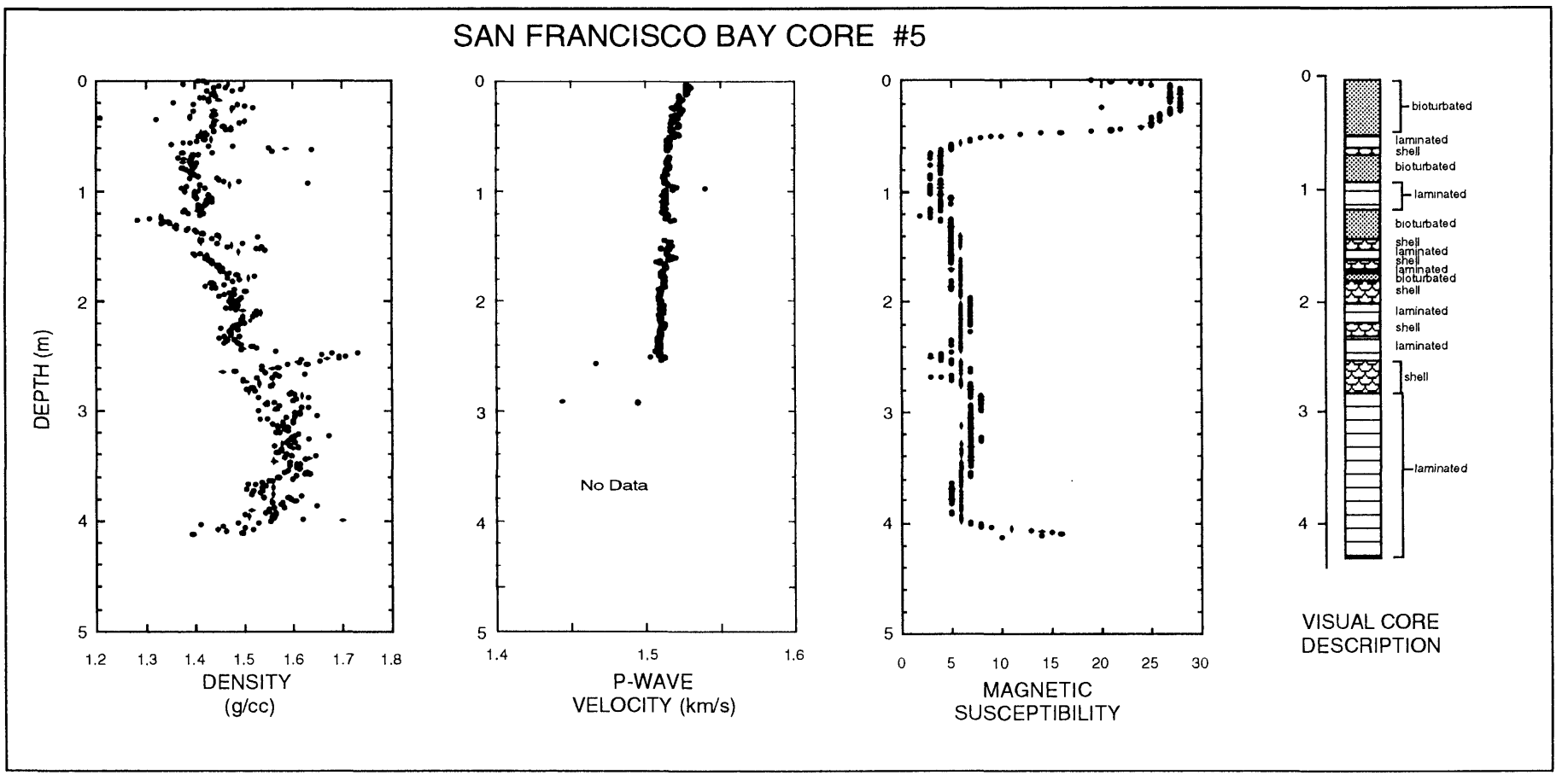
SAN FRANCISCO BAY CORE #5
DEPTH (m)
0
1
2
3
4
5
1.2
1.3
1.4
1.5
1.6
1.7
1.8
DENSITY
(g/cc)
No Data
1.4
1.5
1.6
P-WAVE
VELOCITY (km/s)
0
5
10
15
20
25
30
MAGNETIC
SUSCEPTIBILITY
bioturbated
laminated
shell
bioturbated
laminated
bioturbated
shell
laminated
shell
laminated
bioturbated
shell
laminated
shell
laminated
shell
laminated
VISUAL CORE
DESCRIPTION

Figure 8